^{234}Th sorption and export models in the water column: A review

Nicolas Savoye, Claudia R Benitez-Nelson, Adrian Burd, J. Kirk Cochran, Matthew A Charette, Ken Buesseler, George Jackson, Matthieu Roy-Barman, Sabine Schmidt, Marc Elskens

^{234}Th sorption and export models in the water column: a review

Nicolas Savoye[a]*, Claudia Benitez-Nelson[b], Adrian B. Burd[c], J. Kirk Cochran[d], Matthew Charette[e], Ken O. Buesseler[e], George A. Jackson[f], Matthieu Roy-Barman[g], Sabine Schmidt[h] and Marc Elskens[a]

[a] Dept. of Analytical and Environmental Chemistry, Vrije Universiteit Brussel, B-1050 Brussels, Belgium
[b] Dept. of Geological Sciences, University of South Carolina, Columbia, SC 29208 USA
[c] Dept. of Marine Sciences, University of Georgia, Athens, GA 30602 USA
[d] Marine Sciences Research Center, Stony Brook University, Stony Brook, NY 11794 USA
[e] Dept. of Marine Chemistry and Geochemistry, Woods Hole Oceanographic Institution, Woods Hole, MA 02543 USA
[f] Dept. of Oceanography, Texas A&M University, College Station, TX 77843 USA
[g] LSCE, Domaine du CNRS, F - 91198 Gif-sur-Yvette Cedex, France
[h] Département de Géologie et Océanographie, Université Bordeaux 1, 33405 Talence Cedex, France

* Corresponding author. Now at: OASU UMR CNRS EPOC, Station Marine d'Arcachon 2, rue du Professeur Jolyet, 33120 Arcachon, France TEL : +33 5 56 22 39 16, FAX: +33 5 56 83 51 04, Email : n.savoye@epoc.u-bordeaux1.fr

Abstract

Over the past few decades, the radioisotope pair of $^{238}U/^{234}Th$ has been widely and increasingly used to describe particle dynamics and particle export fluxes in a variety of aquatic systems. The present paper is one of five review articles dedicated to ^{234}Th. It is focused on the models associated with ^{234}Th whereas the companion papers (same issue) are focused on present and future methodologies and techniques (Rutgers van der Loeff et al.), $C/^{234}Th$ ratios (Buesseler et al.), ^{234}Th speciation (Santschi et al.) and present and future applications of ^{234}Th (Waples et al.). In this paper, we review current ^{234}Th scavenging models and discuss the relative importance of the non steady state and physical terms associated with the most commonly used model to estimate ^{234}Th flux. Based on this discussion we recommend that for future work the use of models should be accompanied by a discussion of the effect that model and data uncertainty have on the model results. We also suggest that future field work incorporate repeat occupations of sample sites on time scales of 1-4 weeks in order to evaluate steady state versus non steady state estimates of ^{234}Th export, especially during high flux events (> ca. 800 dpm m^{-2} d^{-1}). Finally, knowledge of the physical oceanography of the study area is essential, particularly in ocean margins and in areas of established upwelling (e.g. Equatorial Pacific). These suggestions will greatly enhance the application of ^{234}Th as a tracer of particle dynamics and flux in more complicated regimes.

Keywords: ^{234}Th, model, scavenging, export, particle dynamics

1. Introduction

Over the past several decades, the decay chains of U and Th have proven extremely useful in describing a wide variety of biological and geological processes. The parent/daughter pair of $^{238}U/^{234}Th$ in particular has been applied to describe particle dynamics and particle export fluxes in a variety of aquatic systems (see the review by Cochran and Masqué, 2003). This is due to several factors, such as 1) ^{238}U is soluble in seawater and behaves conservatively with salinity (Chen et al., 1986), 2) ^{234}Th strongly adsorbs onto particles, and 3) the ^{234}Th half-life of 24.1d allows the study of processes occurring over a time scale of weeks.

^{234}Th measurement techniques, ^{234}Th speciation, and conversion of ^{234}Th flux into carbon and other elemental fluxes are reviewed and detailed in companion papers (see Rutgers van der Loeff et al, Santschi et al, Buesseler et al. and Waples et al., respectively, this issue). Here we focus on the ways in which models have been applied to ^{234}Th data to estimate scavenging rates, residence times, export flux, and particle dynamics. Such models range from the simple (1-box model: Matsumoto, 1975) to the complex (adsorption/aggregation n-box model: Burd et al., 2000). The simplest models require less field data but also give less information and are subject to broad assumptions, e.g., steady state. In contrast, the most complex models require more field data, but are more realistic in terms of predicting actual processes (e.g., Th sorption or transfer from dissolved to particulate phases). The level of model simplicity, e.g., assumptions of steady state or ^{234}Th speciation, ultimately depends on the questions that one aims to answer and the

environmental conditions. At the least, models are very useful tools for making predictions that can be tested in the field.

The goals of this paper are to 1) give an overview of the state of the art for ^{234}Th scavenging models, 2) compare the different assumptions associated with the most commonly used model to estimate ^{234}Th flux, and 3) draw some useful guidelines for researchers who aim to use ^{234}Th as a tracer of particle-associated processes in aquatic systems.

2. Thorium scavenging models- an overview

The development of conceptual and mathematical models of thorium scavenging has been motivated, in part, by the desire to use measurements of thorium deficiencies in surface waters to estimate vertical carbon flux (see Buesseler et al., this volume). The task has been made more difficult by the strong affinity of thorium for all particles, not just those defined as "particulate" by virtue of being caught on a filter of a specified size. Figure 1 shows several different scavenging models that contain different levels of complexity in their representation of particle and sorption dynamics. If thorium scavenging is to be related to particulate organic carbon (POC) export, then additional relationships between particulate thorium, POC concentration, and flux are required. All three of these components are related, but, for the sake of exposition, we shall consider them separately. Here we give a brief review of some of the major types of models that have been and are currently used with ^{234}Th. These models may be classified into two general categories: Sorption and Export. Sorption models consider chemical interactions between thorium in the dissolved and

particulate phases. Export models consider particle interactions that determine the settling velocity and size distribution of the particles.

2.1 Thorium Sorption Models

The sorption and desorption components of a scavenging model describe the chemical nature of the interactions between dissolved and particulate phases. Biologically mediated processes such as remineralization are often considered explicitly, but they have also been implicitly incorporated into some models that describe all transfers between dissolved and particulate phases by a single parameter.

Models of thorium sorption and desorption are often based on the formalism of complexation reactions between metals and particle surfaces (Balistrieri et al., 1981). In this case, the reaction can be expressed by the expression

$$SOH + Me^{z+} \leftrightarrow SOMe^{(z-1)+} + H^{+}$$

where SOH represents a surface –OH group, Me the metal and SOMe the surface ligand-metal ion complex. One proposed adsorption mechanism is that the adsorption process is controlled by the organic content of the particles (Balistrieri et al., 1981; Guo et al., 2002). As with all complexation reactions, modeling these interactions is complicated by their dependence on solution composition, pH, ionic strength, ligand concentration and the concentration of particle surface sites (Honeyman et al., 1988). This basic model has

underpinned most of the research on thorium sorption (*e.g.,* Honeyman et al., 1988; Clegg and Sarmiento, 1989)

Early thorium scavenging models were based on the assumption that thorium produced from the decay of its dissolved parent radionuclide was adsorbed rapidly onto large particles and removed from the system by sedimentation. For example, Balistrieri et al. (1981) developed a model of scavenging using field observations for a number of trace metals, including thorium. They concluded that scavenging was controlled by the organic component of marine particles. Inspired by this, Nozaki et al. (1981) developed a two-box model for ^{230}Th that included specific interactions between the dissolved and particulate thorium pools, but they did not explicitly consider the organic content of the particles. The adsorption rate of dissolved thorium was assumed to be proportional to the dissolved thorium concentration. The reverse transfer from the particulate to dissolved phase was assumed to be proportional to the concentration of particulate thorium. It was acknowledged, however, that this process could involve physical (particle fragmentation), biological (bacterial degradation) and chemical (redox changes in the environment surrounding the particle) processes.

Bacon and Anderson (1982) compared predictions from several different models with deep-sea thorium profiles. These comparisons suggested that the adsorption rate depends on particle concentration. They also demonstrated that the simple two-box model with irreversible uptake was incompatible with deepwater observations where particle concentrations are low. When particle concentrations are high, however, Honeyman et al. (1988) demonstrated that thorium scavenging could be adequately modeled as an irreversible reaction because the reverse rate is negligible when compared to the forward rate. Honeyman

et al. (1988) also showed that the equilibrium distribution coefficients calculated from observed data are strongly dependent on particle concentration.

Despite the successes of these models, the observed scavenging rates in natural waters are much slower than would be predicted using rate constants measured in the laboratory. Santschi et al. (1986) suggested that adsorption to colloids (solid-phase material passing through standard filters) and subsequent aggregation could be an important factor affecting scavenging rates. This mechanism was codified in the Brownian Pumping model (Honeyman and Santschi, 1989; Burd et al., 2000). In this model, the transfer of thorium from a dissolved phase to particles is predominantly or entirely via colloidal intermediates. These are small particles (1 nm to 1 μm) that are not collected using standard filtration techniques. These colloids aggregate to form larger particles, and transfer their adsorbed materials (e.g., Th) into size classes that can be captured on filters. These particles are then further classified as either suspended or sinking particles.

Currently, there is debate about the specific chemistry involved in adsorbing thorium (see Santschi et al., this volume). Guo et al. (2002) argued that thorium in surface waters (upper 75 m) is preferentially adsorbed onto the acid polysaccharide fraction of marine particles. Chase et al. (2002) found that in deep waters thorium was strongly scavenged by carbonate and lithogenic material, but only weakly scavenged by opal. This may reflect changes in the acid polysaccharide content of particulate material with depth, but may also indicate that different processes act at depths, making a model of thorium adsorption for the whole water column more difficult. As these ideas become more fully developed, models of thorium scavenging will have to become more complicated, involving the tracking of

individual chemical components of particulate matter if these models are to describe the ocean's complexity in a realistic manner.

Desorption is generally described mathematically as being proportional to the particulate thorium concentration, independent of particle concentration. However, Quigley et al. (2001) suggested that the adsorption of thorium is, to all practical purposes, irreversible, implying that a "serial adsorption" model may be appropriate.

2.2 Particle Scavenging and Export Models

Thorium export models differ considerably in how they incorporate particle characteristics such as size, settling velocity and lability. These properties are important because thorium flux is determined by the amount of thorium scavenged by particles and the rates at which these particles are removed from the system. The distribution of particulate thorium with particle size depends on the processes of thorium sorption as well as particle aggregation, disaggregation, repackaging by organisms, remineralization and settling. Because particles of different size sink at different speeds, knowledge of the settling speed of individual particles as a function of size, as well as the size dependence of particle concentration, are important for calculating the vertical fluxes.

Two basic factors affect particle settling speeds: the excess density of the particle and the size of the particle. Various regression relationships have been obtained for particle settling speed as a function of particle size (*e.g.,* Alldredge and Gotschalk, 1988, 1989; Syvitski et al., 1995). Modifications of Stokes' Law to incorporate the fractal nature of marine aggregates have been used by Jackson (1995) and Stemmann et al. (2004). These

predict a wide range of settling velocities depending on the particle's excess density and fractal dimension.

The simplest export models combine particulate and dissolved thorium into a single box (Broecker et al., 1973, Matsumoto, 1975, Tanaka et al., 1983; Fig. 1a). In these models, the scavenging rate constant (*k*) incorporates sorption and desorption, aggregation and disaggregation as well as remineralization and particle settling. Such models can be used to give estimates of total thorium residence times but give no information on sorption kinetics or particle dynamics. For example, Broecker et al. (1973) used a global set of measurements of ^{228}Th and ^{228}Ra to determine scavenging rates in coastal regions. It is important to appreciate that in these scavenging models, no particular removal process was specified (adsorption, biological uptake, colloidal interactions).

The general formulation of ^{234}Th activity in the one-box model is the result of a balance between continuous production from ^{238}U, radioactive decay of ^{234}Th, removal onto rapidly sinking particles, and transport into or out of the box by advection and diffusion. The temporal change in total ^{234}Th is expressed by:

$$\frac{\partial A_{Th}}{\partial t} = \lambda A_U - \lambda A_{Th} - P + V \qquad (1)$$

where A_U and A_{Th} are the ^{238}U and the total ^{234}Th activities (expressed in dpm/m^2), respectively, λ is the decay constant of ^{234}Th (= 0.02876 day^{-1}), P (expressed in dpm m^{-2} d^{-1}) is the net removal flux of ^{234}Th, and V is the sum of the advective and diffusive fluxes.

By neglecting physical advection and diffusion (V = 0) and by assuming steady state conditions, i.e. no change of total ^{234}Th activity with time ($\partial A_{Th}/\partial t = 0$), the simple model (Fig. 1a) implies that the net ^{234}Th flux (P) at the base of the layer of interest is equal to the

^{234}Th deficit integrated over depth (A_{Th} - A_U) multiplied by the ^{234}Th decay constant. Thus, eq. 1 is simplified into:

$$P = \lambda(A_U - A_{Th}) \quad (2)$$

The overall uncertainty of P, u(P), assuming the uncertainty of λ is negligible compared to the uncertainties of total ^{234}Th and ^{238}U activities (σ_{ATh} and σ_{Au}, respectively), is given by:

$$u(P) = \lambda\sqrt{\sigma^2_{A_U} + \sigma^2_{A_{Th}}} \quad (3)$$

This formulation of ^{234}Th flux (eq. 2) is by far the most commonly used model in ^{234}Th export studies, due to its simplicity and ease of application (i.e. only total ^{234}Th need be measured).

Two-box models distinguish between dissolved and particulate thorium and thereby include the possibility of understanding the kinetics and dynamics involved. However, as noted above, the "dissolved" fraction usually implicitly includes colloidal particles. Krishnaswami et al. (1976) used a two-box model of deep water ^{230}Th which distinguished dissolved and particulate thorium. Using measurements of deep water ^{230}Th they estimated that particle settling speeds were of the order of 1.7 m d^{-1}. The simple two-box model used by Krishnaswami et al. (1976) is similar to a one-box model used by Bhat et al. (1969) for an analysis of ^{234}Th measurements around Asia and Australia. In this case, surface measurements were used (down to 200 m) and a range of settling velocities from 0.6 to 1.7 m d^{-1} was calculated. These values are generally thought to be unrealistically low since aggregate concentrations display a seasonal signal (Lampitt et al., 1993) that would be hard

to explain with such low sinking rates. This was one concern that led to the use of models with multiple particle size classes.

Bacon and Anderson (1982) compared deep-sea profiles of multiple thorium isotopes (^{230}Th, ^{234}Th, ^{232}Th and ^{228}Th) with profiles predicted by a variety of different models.

These included a two-box (dissolved and particulate thorium) model with irreversible uptake (*e.g.,* Fig 1b with k_{-1}=0), a two-box model with reversible uptake, and a three -box model with irreversible uptake and fast particle removal. None of these models produced depth profiles that agreed well with the observations; in particular none were able to reproduce the observed mid-water maximum in dissolved ^{230}Th. However, they did predict that the thorium sorption rate constant depended on particle concentration and that dissolved ^{230}Th should increase with depth.

A three-box model structure (Fig. 1c) was applied by Clegg and colleagues to observations in the Pacific and North Atlantic (Clegg and Whitfield, 1990, 1991, 1993; Clegg et al., 1991). A particle sinking rate of 150 m d^{-1} was assumed for the North Atlantic Bloom Experiment data and the models were used to infer rate constants such as remineralization, aggregation etc. Various assumptions were made in each case; for example, in the analysis of the NABE data, total suspended particulate matter concentrations were used rather than POC. These authors concluded that the inferred rate constants were not sensitive to the assumed settling velocities.

Forward modeling techniques are used to make predictions given a model structure. In contrast, inverse modeling techniques use the comparison between model results and existing data to tune model parameter values such that model results give the best agreement with the data. Murnane and colleagues used inverse methods to infer rate constants given a

model structure with minimal assumptions about values of constants (Murnane, 1994; Murnane et al., 1990, 1994, 1996). The first model (Murnane et al., 1990) was a three-box model with remineralization from the small particles only. This model predicts generally lower values for the rates of particle aggregation and disaggregation than have others. For the North Atlantic Bloom Experiment, the model did predict much higher rates, similar to those calculated elsewhere. However, the inverse analysis also predicted flux gradients for carbon, nitrogen and total particulates that contrasted with those derived by other means. In addition, the model was modified so that there were two particle pools, one consisting of biogenic material and the other of inert detritus. This permitted the particles to have different labilities (*i.e.,* different rates of degradation). Interestingly, Murnane et al. (1990) appreciated that the model structure they used was a simplification and suggested possible model extensions. These included the fact that particles come in a continuous range of sizes and settling speeds. They also noted that their model would only fit the observed thorium depth profiles if the aggregation and disaggregation rates were functions of depth. Dunne et al. (1997) formulated a similar model, but one in which a phytoplankton component was used to distinguish between reactive and refractory organic particles.

A model directly calculating thorium adsorption onto colloids and larger particles as well as particle aggregation was developed by Burd et al. (2000). Their particle sizes ranged from nano-sized colloids to macroscopic particles. While the theory was developed assuming continuous particle size distributions, its practical application required the size range be sub-divided into a number of particle size classes (Fig 1d) with the particle size distribution and aggregation rates calculated using coagulation. Thorium adsorption and particle settling rates varied with particle size. By specifying the organic carbon content of particles as a function

of particle size, they were able to calculate the size-dependence of the POC/^{234}Th ratio, which was found to decrease as a function of particle size (over a range from nm to mm). Note that thorium was allowed to adsorb onto the whole particle, not just the organic carbon component.

Most of the export models that have been developed either group all particles into a single compartment or else consider a size fractionation between suspended and settling particles only. The boundary between these two groups is often defined operationally by giving a particle size that usually corresponds to a particular filter size. The more detailed, size distribution-based model of Burd et al. (2000) shows how only differentiating between particulate and dissolved material (a "two-box" model) is an oversimplification which can lead to incorrect transfer rates. As an example, we consider a simple coagulation model in which particles of a single size (20 μm diameter) are created at a rate 0.15 d^{-1} and allowed to coagulate and settle out of the water column (the model code can obtained from the following website, http://oceanography.tamu.edu/~Ecomodel/Software/software.html). Calculated settling velocities range between 1 and 275 m d^{-1}. We divide the particle size range (20 μm to 0.1 cm diameter) into two size classes: small and large particles with a size of 50 μm dividing the two. The specific rate of aggregation from small to large particles is calculated to be 0.47 d^{-1}. However, using a simple box model with two particle size classes, together with the above concentrations of small and large particles, we find an aggregation rate of 0.087 d^{-1} and a large particle settling velocity of approximately 20 m d^{-1}.

The calculation above demonstrates that the particle size distribution does indeed matter in determining the rates at which processes occur. Part of the difference between the two calculations arises because each particle size class has its own settling velocity. In

addition, there is a nonlinear concentration distribution of particle sizes that can also affect aggregation rates in a non-linear way. Using a simple first-order reaction rate does not adequately represent the process. Such arguments are not new, but have been raised as potential problems by Murnane et al. (1990) and Burd et al. (2000). Further insight in the consequence of the parameterization of aggregation is obtained from related studies on particle dynamics. While most thorium models are based on linear equations, some marine particle models explicitly use non-linear terms (Athias et al. 2000 a; Dadou et al. 2001). For example, if aggregation of small particles into larger ones is dominated by differential settling, it must be parameterized as a process proportional to both small and large particle concentrations (non-linear term) rather than just as a process proportional small particle concentration (linear term). With the presence of this non-linear term in the equations, the system has a chaotic behavior. This means that if one tries to use particle concentrations and fluxes measured in the water column to determine parameters such as sinking velocities and aggregation - disaggregation rates, a small difference in the concentration or flux values leads to very different sets of velocities and rate constants (Athias et al. 2000a, b). In fact, it is not possible to obtain a single set of parameters as with linear systems but rather a large number of possible solutions exists. In order to constrain this type of dynamic system, it is necessary to obtain thorium data with very high temporal and vertical resolution.

In almost all cases, models have been used to infer rate constants from measured thorium and flux data. Not surprisingly, different model structures give different values for the same apparent rate constants. To date, although there has been analysis of the effects of different inverse techniques, there has been little investigation of model error, i.e. the errors assigned to derived parameters resulting from inaccurate or incorrect model structure. As can

be seen from the simple calculation above with aggregation rates, these errors may be significant.

3. Non-steady state and physical models of ^{234}Th export flux

As noted above, eq. 2 is the simplest representation of ^{234}Th export and is by far the most commonly used. While the model produces a straightforward measure of the ^{234}Th deficit to a given depth, the assumptions of steady state and negligible advection and diffusion are oversimplifications that prevent the effects of blooms, eddies, etc, from being explicitly considered. In practice, each of these assumptions needs to be examined in each situation. In this section, we include the non-steady state and physical terms in the simple model describe above and compare results from some key studies/scenarios.

3.1. Non-steady state (NSS) models

Solving eq. 1 (again neglecting V) when not assuming steady state conditions ($\partial A_{Th}/\partial t \neq 0$) requires the study area and stations to be reoccupied over time. Assuming that P is constant over the time period between two samplings, the solution of eq. 1 is eq. 4. The overall uncertainty, u(P), is given by eq. 5.

$$P = \lambda \left[\frac{A_U (1 - e^{-\lambda \Delta t}) + A_{Th1} e^{-\lambda \Delta t} - A_{Th2}}{1 - e^{-\lambda \Delta t}} \right] \quad (4)$$

$$u(P) = \frac{\lambda}{1 - e^{-\lambda \Delta t}} \sqrt{(1 - e^{-\lambda \Delta t})^2 \sigma^2_{A_U} + e^{-2\lambda \Delta t} \sigma^2_{A_{Th1}} + \sigma^2_{A_{Th2}}} \quad (5)$$

where Δt is the time interval between two occupations of a single station; A_{Th1} and A_{Th2} are the ^{234}Th activities for the first and the second occupations, respectively. Note that this model assumes that the same water mass is sampled both times; thus, ^{238}U activity (A_u) is identical for both visits and advective/diffusive effects are neglected. This assumption should be checked by comparing conservative parameters like salinity, temperature and/or density between visits. It also has the disadvantage of assuming that P is constant between occupations of the station, while in reality P may be changing during this time.

Buesseler et al. (2005) used a different approach to solve eq. 1. They found a linear relationship between A_{Th} and time in the course of the Southern Ocean Iron Experiment (SOFeX) and used its slope to estimate $\partial A_{Th}/\partial t$, and determine P from eq. 1.

3.2 Steady-state versus non-steady state models

A priori the non-steady state model is more accurate since it does not assume that ^{234}Th activity is constant with time. Indeed, such an assumption is often not valid, e.g., during bloom events. Under conditions of sudden export flux, $\partial A/\partial t$ is negative and thus the SS model underestimates the ^{234}Th flux, whereas after the export flux stops, $\partial A/\partial t$ is positive and thus the SS model overestimates the flux. Non-steady state models were used to calculate ^{234}Th flux and/or residence time in eighteen studies between 1983 and 2005. In the following discussion, we compare SS and NSS estimates of ^{234}Th export flux (eq. 2 and 4, respectively) from available data sets (126 data from 12 articles published between 1992 and 2005). This data set represents studies of coastal areas (Wei and Murray, 1992) and the open ocean (Coppola et al., 2005), including studies of eutrophic (Gustafsson et al., 2004), mesotrophic

(Schmidt et al., 2002), oligotrophic (Benitez-Nelson et al., 2001), and high nutrient low chlorophyll (Savoye et al., 2004) areas, from high (Cochran et al., 1995), intermediate (Moran and Buesseler, 1993) and low (Benitez-Nelson et al., 2001) latitudes. It should be noted that the data are not homogeneously distributed over the global ocean as two studies (Buesseler et al., 1998; Gustafsson et al., 2004) account for almost half of the data. Using these data, the ratio of P_{NSS}:P_{SS} (P = ^{234}Th export flux) varies between -2 and 6. This means that assuming SS conditions may overestimate or underestimate the Th export by up to a factor of 6 - 7 (see Rutgers van der Loeff et al., 1997; Gustafsson et al., 2004).

To determine whether differences between P_{NSS} and P_{SS} estimates are statistically significant, a Wilcoxon Signed Rank Test (non parametric alternative to the paired t-test when data are not normally distributed) was applied to the data set. This test enables us to separate the variation due to the model from that due to the variation between samples. It appears that both models provide significantly different results ($p<0.01$). However, when the data are divided into two parts along the median of the P_{SS} data set (median = 800 dpm m^{-2} d^{-1}), there is no significant difference between P_{SS} and P_{NSS} estimates for the lower 50% part of the estimates ($p=0.7$) whereas it is significant for the upper part ($p<0.01$). This means that the difference between the steady state and non steady state fluxes is related to the magnitude of the ^{234}Th export flux: the higher the value of P_{NSS} is, the greater the difference between P_{SS} and P_{NSS}. Thus, the non-steady state model is especially needed during periods of high ^{234}Th export flux, such as the collapse and sinking of a phytoplankton bloom.

Another approach to compare both estimates is to test each pair of estimate (P_{NSS},P_{SS}) as to whether or not the confidence interval (CI) of their absolute difference include zero. CI is defined as: $CI_{|PNSS-PSS|} = k\ (u_{PNSS}^2 + u_{NSS}^2)^{1/2}$, where k is the coverage factor and u denotes

the uncertainty on P_{NSS} and P_{SS} estimates. The value of k is usually taken as two for the 95% confidence level. The null hypothesis that $P_{NSS} = P_{SS}$ is accepted when $|P_{NSS} - P_{SS}| - 95\%CI \leqslant 0 \leqslant |P_{NSS} - P_{SS}| - 95\%CI$. The results of this test, as illustrated by Fig. 2, indicate that 1) there is no significant difference between P_{NSS} and P_{SS} estimates for 75% of the available data, and 2) the results are different depending on the time delay between station occupations (Δt): whereas P_{NSS} and P_{SS} are almost never significantly different when Δt is higher than two half-lives of ^{234}Th, they are significantly different in 45% of the cases when Δt is equal to or lower than one half-life of ^{234}Th (24 days). The first result indicates that, although the steady state assumption is not always valid for ^{234}Th, there are frequent instances in which steady state is approximated. The second set of results is explained by eq. 4: as Δt becomes large, $e^{-\lambda \Delta t}$ tends toward 0, and thus eq. 4 tends toward eq. 2. Clearly, the assumption of constant P_{NSS} when Δt is large is equivalent to an assumption of steady state. Thus, we strongly recommend that future studies attempt to reoccupy stations after a delay of less than one ^{234}Th half-life, especially when fluxes are supposed to be higher than ca. 800 dpm m^{-2} d^{-1}.

3.3 Checking the validity of the steady state assumption

In practice, a steady state model is commonly used to interpret ^{234}Th data because the logistics of most open ocean cruises do not permit stations to be reoccupied. In such cases, it is difficult to test the validity of the steady state assumption. Several studies have shown excesses of ^{234}Th with regard to ^{238}U below the mixed layer, which is interpreted as the result of particle break-up and remineralization (see Waples et al., this issue; Benitez-Nelson et al.,

2001). If physical terms are negligible and assuming steady state, the integrated ^{234}Th excess at depth should be equal to or lower than the integrated ^{234}Th deficit in the upper water column. In other words, release of ^{234}Th at depth due to particle remineralization and break-up should be equal to or lower than ^{234}Th scavenged on the particles sinking from above. This means that mesopelagic ^{234}Th flux should be zero or positive. Negative flux at depth means that the steady state assumption is invalid, when physical terms are negligible. Benitez-Nelson et al. (2001) demonstrated transient remineralization peaks (i.e. negative ^{234}Th fluxes) below depths of 150 m in the North Pacific Subtropical Gyre that equaled in magnitude, after correction for radioactive decay, high ^{234}Th export events from the upper 150m in the preceding months. Savoye et al. (2004) have reported two significantly negative ^{234}Th fluxes at 300m along a latitudinal transect in the Southern Ocean. One station in the transect was reoccupied and a non-steady state model was used to calculate the ^{234}Th flux at 100m. Its comparison with the steady state flux confirms that the steady state assumption was invalid at that site. The calculation of mesopelagic ^{234}Th fluxes appears to be a useful tool for evaluating the steady state assumption. However its usefulness is limited to rejecting the steady state assumption: it cannot be used to validate this assumption since the mesopelagic steady state flux can be positive even if the assumption of steady state is incorrect.

3.4 Uncertainties associated with NSS ^{234}Th export fluxes (P_{NSS})

The usefulness of eq. 4 may be limited by the high sensitivity of the uncertainty of P_{NSS} to the time delay between two visits of a single station (Δt). In order to test this sensitivity, we have simulated variations of ^{234}Th activity for two scenarios and calculated

P_{NSS} and its associated uncertainty for time intervals Δt ranging between 1 and 48 days (i.e. two times the ^{234}Th half life). Scenarios 1 and 2 consider a decrease of ^{234}Th activity of 0.02 dpm/l (i.e. less than usual β-counting uncertainty) and of 0.1 dpm/l, respectively, over Δt. Results of the simulation are illustrated in Fig. 3. It appears that both absolute (error bars on Fig. 3B) and relative (Fig. 3C) uncertainties are very high when Δt is low. The absolute uncertainty is relatively insensitive to the ^{234}Th decrease (error bars of ~2200 dpm/l for Δt = 1 day for both scenarios) and only slightly sensitive to initial ^{234}Th conditions (not shown). In contrast, the relative uncertainty is very sensitive to both the ^{234}Th decrease and initial conditions because P_{NSS} is very sensitive to changes in ^{234}Th activity. Finally, P_{NSS} and its absolute and relative uncertainties are usually only slightly sensitive to a change in ^{238}U (< 0.1 dpm/l; according to Chen et al. (1986), this corresponds to a change in salinity of < 1.4). The exception is when ^{234}Th and ^{238}U are close to secular equilibrium (^{234}Th activity is very close to ^{238}U activity) and Δt > 1 week, i.e. when P_{NSS} is low. Taking into account the high uncertainty in P_{NSS} when Δt is low and the need of revisiting stations within a half life of ^{234}Th (see section 3.2), we recommend that future studies reoccupy select stations after a delay ranging between 1-2 weeks and one ^{234}Th half life.

One option to reduce the high uncertainty due to short Δt is to use an approach similar to that of Buesseler et al. (2005; see section 3.1). Sampling a single station numerous times allows a regression-based estimation of $\partial A_{Th}/\partial t$ and the direct use of eq. 1 for the calculation of P. This approach should be very useful for time series carried out over few weeks, such as in planktonbloom and iron fertilization experiments. Yet even in cases in which the ^{234}Th deficit can be measured at one station over a short period of time, it is important to distinguish between temporal and spatial variability. Submesoscale variations in basic

biology, nutrient distributions and ^{234}Th may obscure the NSS signal. When changes in ^{234}Th profiles are measured over longer times, the likelihood of sampling the same water mass diminishes.

3.5 Incorporating physical transport terms in models of ^{234}Th

In the previous discussion, we have assumed that physical transport ("V" in eq. 1) was negligible. This assumption is often justified in open ocean settings due to minimal advection and diffusion and small gradients in ^{234}Th activities relative to the downward flux of particulate ^{234}Th (P in eq. 1). However, this assumption has become increasingly inappropriate with the expansion of ^{234}Th research to coastal and more dynamic regimes. The physical process term, V (eq. 1), can be expanded to:

$$V = \pm u\frac{\partial A_{Th}}{\partial x} \pm v\frac{\partial A_{Th}}{\partial y} \pm \omega\frac{\partial A_{Th}}{\partial z} \pm K_x\frac{\partial^2 A_{Th}}{\partial x^2} \pm K_y\frac{\partial^2 A_{Th}}{\partial y^2} \pm K_z\frac{\partial^2 A_{Th}}{\partial z^2} \qquad (6)$$

Eq. 6 has both advective and diffusive components. The first three terms include u, v, and w as the velocities in the chosen x, y, and z directions, respectively, and $\delta A_{Th}/\delta x$, $\delta A_{Th}/\delta y$, and $\delta A_{Th}/\delta z$ as the activity gradients along the chosen x,y, and z axis. The second three terms include, K_x and K_y as the x and y horizontal diffusivities, and K_z as the z vertical diffusivity. The second derivative of the activity distribution is described by $d^2A_{Th}/\delta x^2$, $d^2A_{Th}/\delta y^2$, and $d^2A_{Th}/\delta z^2$ in the chosen x, y, and z directions. The relative importance of each term in eq. 6

depends upon the measured $^{234}Th/^{238}U$ disequilibria, the magnitude and sign of the velocity and diffusive fields and the ^{234}Th activity gradients.

In the open ocean, the most common physical process affecting ^{234}Th activity distributions is vertical upwelling of water from depth (Buesseler et al. 1995, 1998; Bacon et al. 1996; Dunne and Murray 1999). This process transports ^{234}Th equilibrium waters into ^{234}Th depleted surface waters, which, in essence, increases the amount of total ^{234}Th available for export. Thus, upwelling will typically result in underestimations of ^{234}Th export if not included. One of the best examples of the effects of upwelling on ^{234}Th distributions is in the Equatorial Pacific, where easterly trade winds drive equatorial divergence and hence upwelling from underlying deep waters.

During the 1992 U.S. JGOFS Process Study of the Equatorial Pacific, Bacon et al (1996) used a 1D model that included profiles of ^{234}Th at the equator and a vertical upwelling term, *w*, that was derived from winds and the model of Philander et al. (1987). Using this model, Bacon et al. (1996) determined ^{234}Th fluxes that were 45 % higher during El-Niño versus non-El Niño conditions. Without the upwelling term, Bacon et al. (1996) would have actually determined lower ^{234}Th deficits and hence, lower ^{234}Th export fluxes during El Niño than those found during non-El Niño conditions.

Also as part of the JGOFS EqPac Process Study, Buesseler et al. (1995) sampled a transect that crossed the high intensity upwelling zone of the equator. Using this data with site specific *u*, *v*, and *w* velocities determined from a wind forced general ocean circulation model configured for the tropical Pacific Ocean (Chai et al. 1996), Buesseler et al. (1995) developed a three dimensional steady-state model to calculate ^{234}Th export fluxes during El Niño (Fig. 4). Using this model, Buesseler et al. (1995) found that ^{234}Th fluxes increased by

almost 50% between 2˚N and 2˚S and were actually slightly lower in regions immediately to the north and south, where down welling occurred. This model further demonstrated that horizontal advection terms were relatively insignificant in the overall ^{234}Th balance.

More recently, Dunne and Murray (1999) used a simplified conceptual model of equatorial circulation (e.g., Philander, 1990) based on a two-dimensional advection stream function of upwelling and meridional recirculation between the equator and 5˚N and 5˚S (patterned after the Chai et al (1996) model used by Buesseler et al. (1995)) (Fig. 5). In this study, it was assumed that zonal advection, i.e $u\ \delta A_{Th}/\delta x$, was negligible, however a diffusive component was added with an assumed diffusion coefficient. Dunne and Murray (1999) also included a particle scavenging model (after Bacon and Anderson (1982)) in order to reduce uncertainties associated with calculating gradients of ^{234}Th versus depth, which often have associated large errors. While this study also found upwelling to play a significant role in ^{234}Th mass balance estimates, this role was mitigated by horizontal diffusion carrying the recently upwelled high activity ^{234}Th away from the equator. In other words, ^{234}Th fluxes were over estimated by 33 % when only advection was considered.

In contrast to the open ocean, the dynamic nature of near shore processes necessitates that physical processes be included whenever possible. Despite the large number of coastal ^{234}Th studies that have been conducted, however, inclusion of physical process terms is rare. The importance of horizontal advection in particular, has plagued coastal ^{234}Th studies for decades. Until recently, evidence for horizontal advection of ^{234}Th has come indirectly. For example, McKee et al. (1984) found that 1-D ^{234}Th fluxes on the Yangtze Continental Shelf did not match underlying ^{234}Th sediment inventories. They used the difference between the two to determine a horizontal transport term that was almost equal in magnitude to the

vertical flux. One of the first direct estimates of horizontal processes on ^{234}Th export rates was conducted by Gustafsson et al. (1998) in Casco Bay, Gulf of Maine. Their 2-D steady state model included both horizontal advection and diffusion perpendicular to shore. Horizontal velocities were estimated using salinity gradients, while the dispersion coefficient was estimated from tides. Net offshore advection was found to be negligible (≤ 2 % in all cases). Horizontal diffusion, however, was substantial in the case of Inner Casco Bay in Spring 1994, with the vertical 1-D steady-state model underestimated the ^{234}Th scavenging flux by > 50% relative to the 2-D model (Fig. 6). In essence, high ^{234}Th activity outer waters diffused into near shore low activity areas and hence, more ^{234}Th export was needed to maintain mass balance. Underlying excess sediment inventories of ^{234}Th provided further evidence that there was significant horizontal onshore transport of ^{234}Th into Inner Casco Bay, with the ratio of ^{234}Th excess relative to the 1-D water column ^{234}Th flux of 340% for Inner Casco Bay and 170% for Outer Casco Bay (Gustafsson et al. 1998). The effects of horizontal advection decreased significantly with increasing distance offshore. Although horizontal diffusion was significant in just one season in the inner harbor, these results illustrate the dynamic nature of the coastal system and its potential impact on ^{234}Th export determinations.

Benitez-Nelson et al. (2000) conducted a similar study in the Gulf of Maine, but further offshore in Wilkinson Basin. A non-steady state term was also included. Both along shore and off shore horizontal advection velocities were determined using historical current meter measurements, and although alongshore current velocities were significantly greater than offshore (5-13 cm s^{-1} versus 1 cm s^{-1}), there was little change in ^{234}Th activities along the coast. As a result, there was little to no ^{234}Th advective or diffusive transport parallel to

shore. Horizontal diffusion estimates were obtained using Okubo's (1971) empirically derived oceanic diffusion diagrams. Using a 2-D model, Benitez-Nelson et al. (2000) found that offshore advection and diffusion of ^{234}Th decreased ^{234}Th fluxes significantly, particularly in late summer when offshore gradients in ^{234}Th activities were highest (Fig. 7). In this case, the offshore advective term reflects the transport of low ^{234}Th activity waters to areas of higher activity. This low ^{234}Th activity results in the 'appearance' of more particulate export than what actually occurred. Although the advective term is counteracted by diffusion, diffusion tended to be less than 25 % of the advective component. As a result, the advection/diffusion term in Fig. 7 is negative.

It is important to note how sensitive ^{234}Th export fluxes are to the chosen current velocities, horizontal diffusion coefficients, and measured ^{234}Th activity gradients for any study that includes physical process terms. For example, in the 2-D model used by Benitez-Nelson et al. (2000), doubling the advective offshore current velocity, v, results in a decrease in the ^{234}Th export flux by greater than 50 % in April and July, and by greater than 250 % in August. In contrast, doubling the horizontal eddy diffusivity, K_y, increases the ^{234}Th export flux by less than 30%. Increasing or decreasing the first and second order activity gradients (e.g., $\delta A_{Th}/\delta x$ and $\delta^2 A_{Th})/\delta x^2$) results in similar magnitude changes in the ^{234}Th export for all three months.

Most recently, Charette et al. (2001) evaluated the impact of horizontal advective and diffusive transport on the ^{234}Th export flux in the northeastern Gulf of Maine using a 3-D model. Physical transport parameters were obtained from the three dimensional non-linear Princeton Ocean Model applied to the Gulf of Maine (see Xue et al., 2000). In many cases there was no statistical difference in the ^{234}Th flux derived from either the 1-D or 3-D model,

and inclusion of horizontal advective and diffusive components only increased ^{234}Th export by an overall average of 10 % relative to the traditional 1-D model. However, individual stations demonstrated significant differences between the 1-D and the 3-D model depending on their location (Fig. 8). For example, the 3-D model predicts a 100% higher ^{234}Th flux at Sta. 10 relative to the 1-D model, a function of both the large gradient in ^{234}Th (1.8 dpm L^{-1} to 1.2 dpm L^{-1} from Sta. 10 to Sta. 11) and the strong currents that move into the Gulf through the Northeast Channel. A similar effect was also evident at Sta. 27, due to its proximity to low ^{234}Th activities on Georges Bank. In contrast, at Sta. 17 and 22 where ^{234}Th activities increased along the flow path of the Maine Coastal Current, the 3-D model predicted a 33% reduction in the ^{234}Th flux relative to the 1-D model.

In the application of ^{234}Th in aquatic systems, one of the key issues is determining when physical processes should be incorporated. This in turn is a function of the magnitude of export (or P in eq. 1), the current velocity, and the gradient in ^{234}Th activities over the depth scale of interest. For example, Charette et al. (2001) noted that the contribution of the advection component to the Th export flux typically decreased with depth. This is predominantly due to a decrease in the current velocity, which tends to decrease with depth as well. Although complicated, we can begin to use simple models to determine when physical processes should be included. For example, oligotrophic settings typically have ^{234}Th export fluxes that range between 500 -1000 dpm ^{234}Th m^{-2} d^{-1}. Let's assume that small net changes in export (e.g., $\leq$ 100 dpm ^{234}Th m^{-2} d^{-1}) occur over a distance of 100 km and a typical open ocean current speed of 1 cm s^{-1} (integrated over the entire upper 150 m). Not including the physical process term would put export fluxes in error by less than a 15 %. However, if the current speed where to increase to 10 cm s^{-1} (say in a strong current like the

Gulf Stream), the error in export calculations would increase to ~ 50 %. If initial export fluxes were typical of more productive regions, e.g., > 3000 dpm ^{234}Th m^{-2} d^{-1} (Buesseler 1998), then at current speeds of 10 cm s^{-1}, export fluxes would be in error by less than 20 %. If the horizontal gradient in ^{234}Th activity was increased, i.e. a change of 300 dpm ^{234}Th m^{-2} d^{-1} over a distance of 100 km, and physical processes ignored, then the export flux would be in error of ~ 40 % in a regime with a horizontal current velocity of 1 cm s^{-1} and low export or ~ 50 % at 10 cm s^{-1} and high export.

The above open ocean and coastal studies have provided a basis for future research using ^{234}Th in aquatic ecosystems. In essence, differences between 1-D and 2-D/3-D approaches are greatest where current velocities are high and ^{234}Th gradients large. In the open ocean, the physical process of upwelling, although offset by horizontal advection and diffusion, appears to be the dominant physical process. In the coastal ocean, horizontal advective and diffusive terms must be considered. In the end, however, all physical models of ^{234}Th are greatly dependent on the accuracy of the fluid field in which the study occurs.

4. Summary and Recommendations

The interpretation of ^{234}Th distributions in aquatic systems requires a synthesis of laboratory and field data and the application of models that help set the data in the context of natural processes. In this manner, predictions can be made that direct future applications of particle export and particle dynamics using ^{234}Th. Perhaps the most difficult aspect in obtaining this synthesis, however, is matching the complexity of the model and constraining model parameters with the ability to make appropriate measurements. Although adding

complexity to models may better approximate the natural environment, it is important to note that complex models in themselves are not necessarily "correct" or better than simple models. At one level or another, however, models govern our interpretation of ^{234}Th data in the aquatic environment. Indeed, even the simplest estimation of a sinking ^{234}Th flux from its deficit relative to ^{238}U through a given depth horizon (e.g., eq. 2) is model-driven (one-box model, assuming steady state and negligible physical transport). Using this ^{234}Th flux to derive POC fluxes requires a further set of assumptions (and models) regarding the link between POC and ^{234}Th that add complexity (and uncertainty) to the final result (see Buesseler et al., this volume).

Like experimental and field data, both forward and inverse modeling techniques involve uncertainties. Forward, predictive models suffer from uncertainty in the parameter values used and in the formulation of the model itself (e.g., which process to include and which ones to neglect). For example, the model results of Dunne et al. (1997) were strongly affected by the sampling methodology used to collect the data utilized in the model. Buesseler et al. (1995) and Dunne and Murray (1999) showed that better agreement between model results and data were obtained when vertical advection was included in the model formulation. Similarly, uncertainties in field data and model formulation, as well as choice of modeling technique, affect parameter values derived using inverse techniques. Murnane et al. (1994) showed different least squares techniques give different values for model rate parameters such as thorium adsorption and desorption rates and particle aggregation and disaggregation rates. Our calculations show that the non-linearity of the particle size distribution affects aggregation and settling rates predicted from a forward model. The use of

forward and inverse models should be accompanied by a discussion of the effect that model and data uncertainty have on the model results.

A critical source of uncertainty in ^{234}Th export models used to estimate ^{234}Th fluxes from the water column is the assumption of steady state and minimal physical processes. The steady state assumption may be checked by repeated occupations of a single station to determine the extent to which the ^{234}Th deficit changes with time. This is especially important when fluxes are expected to be higher than ca. 800 dpm m^{-2} d^{-1}. Our analysis of uncertainties associated with estimates of non-steady state Th flux suggests that the uncertainty is high over short time periods (e.g., few days) between reoccupations. We recommend that reoccupation on a time scale of 1 – 4 weeks is the most appropriate for evaluation of non-steady state. Some oceanographic expeditions are organized in a fashion that is amenable to such an approach (e.g., the iron fertilization experiments, time-series) and some are clearly not. To the extent possible, however, we recommend that non-steady state aspects of ^{234}Th profiles be evaluated, particularly in situations such as blooms, when the flux of particulate material (and ^{234}Th) is changing on a time scale similar to the half-life of ^{234}Th.

Physical processes also affect ^{234}Th profiles, and may range from relatively unimportant in central gyre regions to dominant in ocean margins. Knowledge of the physical oceanography of an area is essential. For example, areas of established upwelling, such as the Equatorial Pacific, need to have this process incorporated into all models of ^{234}Th. In ocean margin settings, advection and diffusion are likely important. As such, in these areas, measurement of the spatial gradients in ^{234}Th/^{238}U disequilibrium is useful in evaluating the importance of lateral transport.

Combined, modeling and measurements of ^{234}Th have provided powerful insights into particle scavenging and the processes that control reactive element uptake and removal from the oceans. The development of new techniques (Rutgers van der Loeff et al. this issue) and the application of ^{234}Th to new research avenues (Waples et al., this issue) will continue to impact the field of oceanography. As such, the complexity of models currently used in ^{234}Th applications needs to be reevaluated and new modeling and measurement studies enacted which can continue to expand upon the wealth of information already gained by the aquatic community over the past half-century.

Acknowledgements

This paper grew out of discussion held at the "Future Applications of ^{234}Th in Aquatic Systems" workshop held at Woods Hole Oceanographic Institution in August, 2004 (see: http://www.geol.sc.edu/cbnelson/Thmeeting/). We are grateful to the US National Science Foundation Chemical Oceanography Program (OCE 0354757) for its support of the workshop. Kanchan Maiti (Univ. of South Carolina) and Paul Morris (Southampton Oceanography Centre) served as rapporteurs for the modeling discussions and we thank them for their efforts. We thank John Dunne and one anonymous reviewer for their comments and suggestions leading to improve the quality of the paper, as well as Bob Anderson as guest editor of this paper. Finally we thank the US National Science Foundation, the National Oceanic and Atmospheric Administration and the Belgian Science Policy for their support of many of the field and modeling efforts described in this paper.

References

Alldredge, A.L. and Gotschalk, C., 1988. In situ settling behavior of marine snow. Limnology and Oceanography 33:339-351.

Alldredge, A.L. and Gotschalk, C.C., 1989. Direct observations of the flocculation of diatom blooms: characteristics, settling velocity, and formation of diatom aggregates. Deep-Sea Research I, 36:159-171.

Athias, V., Mazzega, P. and Jeandel, C., 2000a. Nonlinear inversions of a model of the oceanic dissolved-particulate exchanges. In: Kasibhatla, P., Heimann, M., Rayner, P., Mahowald, N., Prinn, R., Hartley, D. (Eds.), Inverse Methods in Global Biogeochemical Cycles, Geophysical Monograph Vol.114, AGU, pp.205-222.

Athias, V., Mazzega, P. and Jeandel, C., 2000b. Selecting a global optimization method to estimate the oceanic particle cycling rate constants, Journal of Marine Research, 58:675-707.

Bacon, M.P. and Anderson, R.F., 1982. Distribution of thorium isotopes between dissolved and particulate forms in the deep sea. Journal of Geophysical Research 87:2045-2056.

Bacon, M.P., Cochran, J.K., Hirschberg, D., Hammar, T.R. and Fleer, A.P., 1996. Export flux of carbon at the equator during the EqPac time-series cruises estimated from ^{234}Th measurements. Deep-Sea Research II, 43 (4-6):1133-1153.

Balistrieri, L., Brewer, P.G. and Murray, J.W., 1981. Scavenging residence times of trace metals and surface chemistry of sinking particles in the deep ocean. Deep-Sea Research, 28:101-121.

Benitez-Nelson, C., Buesseler, K.O. and Crosselin, G., 2000. Upper ocean carbon export, horizontal transport, and vertical eddy diffusivity in the southwestern Gulf of Maine. Continental Shelf Research, 20:707-736.

Benitez-Nelson, C., Buesseler, K.O., Karl, D.M. and Andrews, J., 2001. A time-series study of particulate matter export in the North Pacific Subtropical Gyre based on ^{234}Th:^{238}U disequilibrium. Deep-Sea Research I, 48:2595–2611.

Bhat, S.G., Krishnaswami, S., Lal, D., Rama, D. and Moore, W.S., 1969. $^{234}Th/^{238}U$ ratios in the ocean. Earth and Planetary Science Letters, 5:483-491.

Broecker, W.S., Kaufman, A. and Trier, R.M., 1973. The residence time of thorium in surface sea water and its implication regarding the rate of reactive pollutants. Earth. and Planetary Science Letters, 20:35-44.

Buesseler, K.O., 1998. The de-coupling of production and particulate export in the surface ocean. Global Biogoechemical Cycles, 12 (2), 297-310.

Buesseler, K.O., Andrews, J.A., Hartman, M.C., Belastock, R. and Chai, F., 1995. Regional estimates of the export flux of particulate organic carbon derived from thorium-234 during the JGOFS EqPac program. Deep-Sea Research II, 42:777-804.

Buesseler, K.O., Andrews, J.E., Pike, S.M., Charette, M.A., Goldson, L.E., Brzezinski, M.A. and Lance, V.P., 2005. Particle export during the Southern Ocean Iron Experiment (SOFeX). Limnology and Oceanography, 50 (1):311-327.

Buesseler, K., Ball, L., Andrews, J., Benitez-Nelson, C., Belastock, R., Chai, F. and Chao, Y., 1998. Upper ocean export of particulate organic carbon in the Arabian Sea derived from thorium-234. Deep-Sea Research II, 45:2461-2487.

Buesseler, K.O., Ball, L., Andrews, J., Cochran, J.K., Hirschberg, D.J., Bacon, M.P., Fleer, A. and Brzezinski, M., 2001. Upper ocean export of particulate organic carbon and biogenic silica in the Southern Ocean along 170°W. Deep-Sea Research II, 48 (19-20):4275-4297.

Buesseler, K.O., Benitez-Nelson, C.R., Moran, S.B., Burd, A., Charette, M., Cochran, J.K., Coppola, L., Fisher, N.S., Fowler, S.W., Gardner, W.D., Guo, L.D., Gustafsson, Ö., Lamborg, C., Masque, P., Miquel, J.C., Passow, U., Santschi, P.H., Savoye, N., Stewart, G., and Trull, T., accepted. An assessment of particulate organic carbon to thorium-234 ratios in the ocean and their impact on the application of ^{234}Th as a POC flux proxy. Marine Chemistry, FATE special issue.

Burd, A.B., Jackson, G.A. and Moran, S.B., 2000. A coupled adsorption-aggregation model for the POC/^{234}Th ratio of marine particles. Deep-Sea Research I, 47:103-120.

Chai F., Lindley, S.T. and Barber, R.T., 1996. Origin and maintenance of high nitrate condition in the equatorial Pacific. Deep-Sea Research II, 43 (4-6), 1031-1064.

Charette, M.A., Moran, S.B., Pike, S.M. and Smith, J.N., 2001. Investigating the carbon cycle in the Gulf of Maine using the natural tracer thorium 234. Journal of Geophysical Research, 106 (C6):11,553-11,579.

Chase, Z., Anderson, R.F., Fleisher, M.Q. and Kubik, P.W., 2002. The influence of particle composition and particle flux on scavenging of Th, Pa and Be in the ocean. Earth and Planetary Science Letters, 204:215-229.

Chen, J.H., Edwards, R.L. and Wasserburg, G.J., 1986. ^{238}U, ^{234}U and ^{232}Th in seawater. Earth and Planetary Science Letters, 80:241-251.

Clegg, S.L., Bacon, M.P. and Whitfield, M., 1991. Application of a generalized scavenging model to thorium isotope and particle data at equatorial and high-latitude sites in the Pacific Ocean. Journal of Geophysical Research, 96:20655-20670.

Clegg, S.L. and Sarmiento, J.L., 1989. The hydrolytic scavenging of metal ions by marine particulate matter. Progress in Oceanography, 23:1-21.

Clegg, S.L. and Whitfield, M., 1990. A generalised model for the scavenging of trace metals in the open ocean: I, Particle cycling. Deep-Sea Research, 37:809-832.

Clegg, S.L. and Whitfield, M., 1991. A generalised model for the scavenging of trace metals in the open ocean: II, Thorium scavenging. Deep-Sea Research, 38:91-120.

Clegg, S.L. and Whitfield, M., 1993. Application of a generalized scavenging model to time series ^{234}Th and particle data collected during the JGOFS North Atlantic Bloom Experiment. Deep-Sea Research I, 40:1529-1545,

Cochran, J.K., Barnes, C., Achman, D. and Hirschberg, D.J., 1995. Thorium-234/Uranium238 disequilibrium as an indicator of scavenging rates and particulate organic carbon fluxes in the northeast water polynia, Greenland. Journal of Geophysical Research, 100 (C3):4399-4410.

Cochran, J.K., Buesseler, K.O., Bacon, M.P., Wang, H.W., Hirschberg, D.J., Ball, L., Andrews, J., Crossin G. and Fleer, A., 2000. Short-lived thorium isotope (^{234} Th, ^{228} Th) as indicators of POC export and particle cycling in the Ross Sea, Southern Ocean. Deep-Sea Research II, 47:3451-3490.

Cochran, J.K. and Masqué, P., 2003. Short-lived U/Th series radionuclides in the ocean: tracers for scavenging rates, export fluxes and particle dynamics. In: Bourdon, B., Henderson, G.M., Lundstrom, C.C., Turner, S.P. (Eds.), Uranium-Series Geochemistry. Reviews in Mineralogy & Geochemistry, Vol. 52., pp. 461-492.

Coppola, L., Roy-Barman, M., Muslow, S., Povinec, P. and Jeandel, C., 2005. Low particulate organic carbon export in the frontal zone of the Southern Ocean (Indian Sector) revealed by ^{234}Th. Deep-Sea Research I, 52:51-68.

Dadou, I, Lamy, F., Rabouille, C., Ruiz-Pino, D., Anderson, V., Biamchi, M. and Garcon, V., 2001. An integrated biological pump model from the euphotic zone to the sediment: a 1-D application in the Northeast tropical Atlantic. Deep-Sea Research II, 48:2345-2381.

Dunne, J.P. and Murray, J.W., 1999. Sensitivity of ^{234}Th export to physical processes in the central equatorial Pacific. Deep-Sea Research I, 46:831-854.

Dunne, J.P., Murray, J.W., Young, J., Balistrieri, L.S. and Bishop, J., 1997. ^{234}Th and particle cycling in the central equatorial Pacific. Deep-Sea Research II, 44:2049-2083.

Guo L., Hung, C-C., Santschi P.H. and Walsh, I.D., 2002. ^{234} Th scavenging and its relationship to acid polysaccharide abundance in the Gulf of Mexico. Marine Chemistry, 78:103-119.

Gustafsson, Ö., Andersson, P., Roos, P., Kukulska, Z., Broman, D., Larsson, U., Hajdu, S. and Ingri, J. 2004. Evaluation of the collection efficiency of upper ocean sub-photic-layer sediment traps: a 24-month in situ calibration in the open Baltic Sea using ^{234}Th. Limnology and Oceanography: Method, 2:62–74.

Gustafsson, Ö., Buesseler, K.O., Geyer, W.R., Moran, S.B. and Gschwend, P.M., 1998. An assessment of the relative importance of horizontal and vertical transport of particle-reactive chemicals in the coastal ocean. Continental Shelf Research, 18:805-829.

Honeyman, B.D, Balistrieri, L.S. and Murray, J.W., 1988. Oceanic trace metal scavenging: the importance of particle concentration. Deep-Sea Research, 35:227-246.

Honeyman, B.D. and Santschi, P.H., 1989. A Brownian-pumping model for oceanic trace-metal scavenging: evidence from Th isotopes. Journal of Marine Research, 47:951-992.

Jackson, G.A., 1995. Comparing observed changes in particle size spectra with those predicted using coagulation theory. Deep Sea Research II, 42:159-184.

Krishnaswami, S., Lal, D., Somayajulu, B.K.L., Weiss, R.F. and Craig, H., 1976. Large-volume in-situ filtration of deep Pacific waters: mineralogical and radioisotope studies. Earth and Planetary Science Letters 32:420-429.

Lampitt, R.S., Hillier, W.R. and Challenor, P.G., 1993. Seasonal and diel variation in the open ocean concentration of marine snow aggregates. Nature, 362:737-739.

McKee, B.A., DeMaster, D.J. and Nittrouer, C.A., 1984. The use of $^{234}Th/^{238}U$ disequilibrium to examine the fate of particle-reactive species on the Yangtze continental shelf. Earth and Planetary Science Letters, 68:431-442.

Matsumoto, E., 1975. ^{234}Th-^{238}U radioactive disequilibrium in the surface layer of the ocean. Geochimica et Cosmochimica Acta, 39:205-212.

Moran, S.B. and Buesseler, K.O., 1993. Size-fractionated ^{234}Th in continental shelf waters off New England: Implications for the role of colloids in oceanic trace metal scavenging. Journal of Marine Research, 51:893-922.10

Murnane, R.J., 1994. Determination of the thorium and particulate matter cycling parameters at station P: A reanalysis and comparison of least squares techniques. Journal of Geophysical Research, 99:3393-3405.

Murnane, R.J., Cochran, J.K., Buesseler, K.O. and Bacon, M.P., 1996. Least-square estimates of thorium, particle, and nutrient cycling rate constants from the JGOFS North Atlantic Bloom Experiment. Deep-Sea Research I, 43:239-258.

Murnane, R.J., Cochran, J.K. and Sarmiento, J.L., 1994. Estimates of particle- and thorium-cycling rates in the northwest Atlantic Ocean. Journal of Geophysical Research, 99:3373-3392.

Murnane, R.J., Sarmiento, J.L. and Bacon, M.P., 1990. Thorium isotopes, particle cycling models, and inverse calculations of model rate constants. Journal of Geophysical Research, 95:16195-16206.

Nozaki, Y., Horibe, Y. and Tsubota, H., 1981. The water column distributions of thorium isotopes in the western North Pacific. Earth and Planetary Science Letters, 54:203-216.

Okubo, A., 1971. Oceanic diffusion diagrams. Deep-Sea Research, 18:789-802.

Philander, S. G., 1990. El Niño, La Niña and the Southern Oscillation. Academic Press, New York, 286pp.

Philander S.G.H., Hurlin, W.J. and Seigel, A.D., 1987. Simulation of the seasonal cycle of the tropical Pacific Ocean. Journal of Physical Oceanography, 17:1986-2002.

Quigley, M.S., Santschi, P.H., Guo, L. and Honeyman, B.D., 2001. Sorption irreversibility and coagulation behavior of ^{234}Th with marine organic matter. Marine Chemistry, 76:27-45.

Rutgers van der Loeff, M.M., Friedrich, J. and Bathmann, U.V., 1997. Carbon export during the spring bloom at the Antarctic Polar Front, determined with the natural tracer ^{234}Th. Deep-Sea Research II, 44 (1-2):457-478.

Rutgers van der Loeff, M., Sarin, M.M., Baskaran, M., Benitez-Nelson, C., Buesseler, K.O., Charette, M., Dai, M., Gustafsson, Ö., Masque, P., Morris, P., Orlandini, K., Rodriguez y Baena, A., Savoye, N., Schmidt, S., Turnewitsch, R., Vöge, I. and Waples, J., accepted. A review of present techniques and methodological advances in analyzing ^{234}Th in aquatic systems. Marine Chemistry, FATE special issue.

Santschi, P.H., Murray, J.W., Baskaran, M., Benitez-Nelson, C.R., Guo, L.D., Hung, C.-C., Lamborg, C., Moran, S.B., Passow, U. and Roy-Barman, M., accepted. Thorium speciation in seawater. Marine Chemistry, FATE special issue.

Santschi, P.H., Nyffeler, U.P., Li, Y.-H. and O'Hara, P., 1986. Radionuclide cycling in natural waters: relevance of scavenging kinetics. In: Syl, P.G. (Ed.), Sediments and Water Interactions. Springer-Verlag, New York, chapter 17, pp. 183-191.

Savoye, N., Buesseler, K.O., Cardinal, D. and Dehairs, F., 2004. ^{234}Th deficit and excess in the Southern Ocean during spring 2001: particle export and remineralization. Geophysical Research Letters, 31, L12301, doi: 10.1029/2004GL019744.

Schmidt, S., Andersen, V., Belviso, S. and Marty, J.-C., 2002. Strong seasonality in particle dynamics of north-western Mediterranean surface waters as revealed by ^{234}Th/^{238}U. Deep-Sea Research I, 49:1507-1518.

Stemmann, L., Jackson, G.A. and Ianson, D., 2004. A vertical model of particle size distributions and fluxes in the midwater column that includes biological and physical processes – Part I: model formulation. Deep-Sea Research I, 51:865-884

Syvitski, J.P.M., Asprey, K.W. and Leblanc, K.W.G., 1995. In situ characteristics of particles settling within a deep-water estuary. Deep-Sea Research II, 42:223-256.

Tanaka, N., Takeda, Y. and Tsunogai, S., 1983. Bioloical effect of removal of Th-234, Po-210 and Pb-210 from surface water in Funka Bay, Japan. Geochimica et Cosmochimica Acta, 47:1783-1790.

Waples, J. T., Benitez-Nelson, C.R., Savoye, N., Rutgers van der Loeff, M., Baskaran, M., Gustafsson, Ö. An Introduction to the application and future use of ^{234}Th in aquatic systems. Marine Chemistry, FATE special issue.

Wei, C.L. and Murray, J.W., 1992. Temporal variations of ^{234}Th activity in the water column of Dabob Bay: particle scavenging. Limnology and Oceanography, 37 (2):296-314.

Xue, H., Chai, F. and Pettigrew, N.R., 2000. A model study of seasonal circulation in the Gulf of Maine. Journal of Physical Oceanography, 30, 1111-1135.

Figure captions

Fig. 1: Schematic of the major classes of thorium scavenging model. U represents the uranium activity with λ_U being the decay constant for the uranium isotope. Decay of thorium is represented by λ_{Th} and the settling rate of particulate material by S. a) One-box model with the total thorium (Th_T) being the sum of dissolved and particulate. A total scavenging rate constant (*k*, representing uptake onto particles and particle sinking,) is given in this model. b) Two-box model with dissolved and particulate thorium (Th_d and Th_p respectively) explicitly represented. The rate constants k_1 and k_{-1} represent adsorption and desorption of thorium. Note however, that desorption of thorium in this model actually includes all process that transfer thorium from the particulate to the dissolved phase (desorption, remineralization etc.). c) Three-box model where the particulate phase is divided into small (non-settling) particles and large (settling) particles. The rate constants k_2 and k_{-2} represent aggregation and disaggregation rates between these compartments. In addition, γ represents the remineralization of particulate material. d) This model contains an explicit representation of the particle size distribution. It includes n+1 boxes and represents dissolved thorium and n particle size class. Thorium can be adsorbed and desorbed from each particle size class, and particles in each size class have a settling rate. Thorium can be transferred between size classes by particle aggregation.

Fig. 2: Illustration of the a statistical test applied to the available literature data sets in order to determine if the estimates of steady and non-steady state ^{234}Th export fluxes (P_{SS} and P_{NSS}, respectively) are or are not significantly different at the 0.05 level. Δt is the time delay

between two visits of a single station. abs($P_{NSS} - P_{SS}$) – 95%CI is positive or negative when the difference between the estimates is or is not significant (at the 0.05 level), respectively. CI is the confidence interval of abs($P_{NSS} - P_{SS}$) (see section 3.2 for details).

Fig. 3: Sensitivity of NSS ^{234}Th export flux to the time delay between two visits of a single station (Δt). A: activity profiles of total ^{234}Th (symbols) and ^{238}U (no symbol). B: NSS ^{234}Th export flux versus Δt; error bars correspond to the absolute uncertainty. C: relative uncertainty of the NSS ^{234}Th export flux versus Δt. The ^{234}Th flux and its uncertainty are calculated according to eqs. 4 and 5, respectively. Uncertainties of ^{234}Th and ^{238}U activities used for the calculation of the propagated error are 2% (usual counting error) and 1%, respectively. Initial conditions for ^{234}Th activity and ^{238}U activity are typical for spring/summer Southern Ocean. Scenario 1 and 2 correspond to a decrease of the ^{234}Th activity of 0.02 dpm/l (i.e. less than usual counting uncertainty) and 0.1 dpm/l, respectively.

Fig. 4: Comparison of the individual flux terms calculated from the 3-D model along a transect across the equator in Fall 1992. Total ^{234}Th fluxes are shown by the shaded panel. A non-advective model (flux = $(A_U - A_{Th})/\lambda$) predicts lower fluxes near the equator (filled squares). Advective ^{234}Th fluxes are calculated for upwelling ($w\ \delta A_{Th}/\delta z$, open squares) and horizontal advection ($u\ \delta A_{Th}/\delta x$, open circles, $v\ \delta A_{Th}/\delta y$, filled circles). All fluxes are in dpm ^{234}Th m^{-2} d^{-1}. Figure taken from Buesseler et al. (1995).

Fig. 5: Model contours of total ^{234}Th (dpm $m^{\sim 3}$) between 5˚N and 5˚S in the upper 250 m (A) without advection or diffusion, (B) with diffusion only, (C) with advection only, and (D) with both advection and diffusion. Figure taken from Dunne and Murray (1999).

Fig. 6: Comparison of 1-D (vertical hatched bars) and 2-D (diagonal hatched bars) ^{234}Th flux models for Inner and Outer Casco Bay. The error bars (± 1σ) represent propagated uncertainties from ^{234}Th counting statistics. Figure redrawn from Gustafsson et al. (1998).

Fig. 7: 2-D ^{234}Th model flux results. Each stacked bar represents the magnitude of the steady-state term ((A_U-A_{Th})λ; white), non-steady state term ((δA_{Th})/δdt; black) and advection + diffusion terms (u $\delta A_{Th}/\delta x + K_x \delta^2 A_{Th}/\delta x^2$; light gray). The net ^{234}Th fluxes (black circles) from the inclusion of all three terms are also shown. All fluxes were integrated over the upper 10 m and are in dpm m^{-2} d^{-1}. Boxes 1 and 3 are inshore, and 2 and 4 are offshore. Overall errors are determined from the average uncertainties associated with ^{234}Th collection efficiencies and counting statistics. Possible errors derived from current velocities and diffusion coefficients were not included. Figure from Benitez-Nelson et al. (2000).

Fig. 8: Comparison of steady-state 1-D and 3-D ^{234}Th fluxes for the Gulf of Maine/Scotia Shelf region during September 1997. The error bars (+/- 1 sigma) represent propagated uncertainties from ^{234}Th counting statistics and thus, do not include an estimate of the uncertainty associated with the horizontal dispersion and net advection transport parameters. Station locations and other details can be found in Charette et al. (2001).

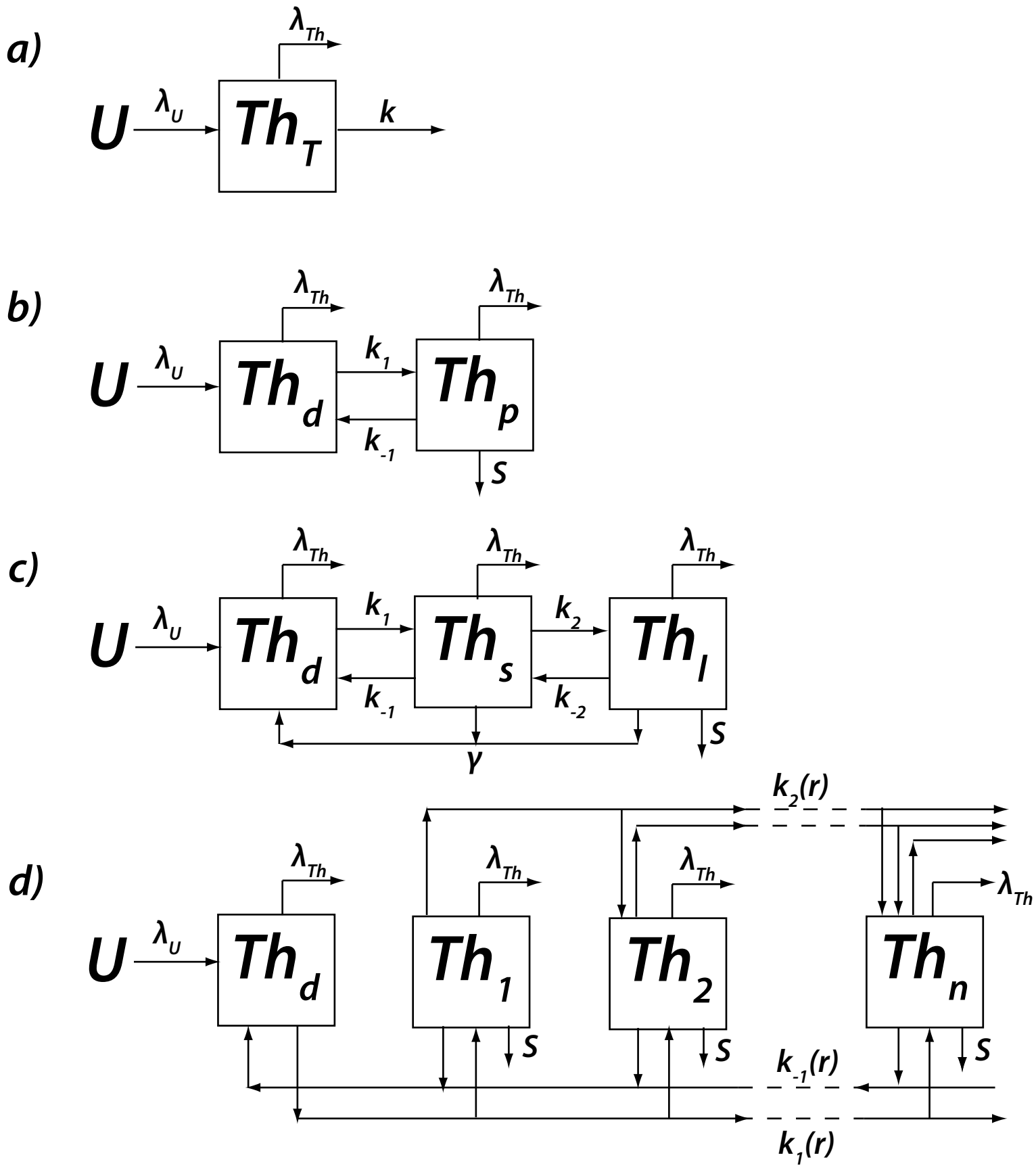
a)
λTh
U
λU
Th T
k
b)
λTh
λTh
U
λU
Th d
k1
Th p
k-1
s
c)
λTh
λTh
λTh
U
λU
Th d
k1
Th s
k2
Th l
k-1
k-2
s
γ
d)
k2(r)
λTh
λTh
λTh
λTh
U
λU
Th d
Th 1
Th 2
Th n
s
s
s
k-1(r)
k1(r)

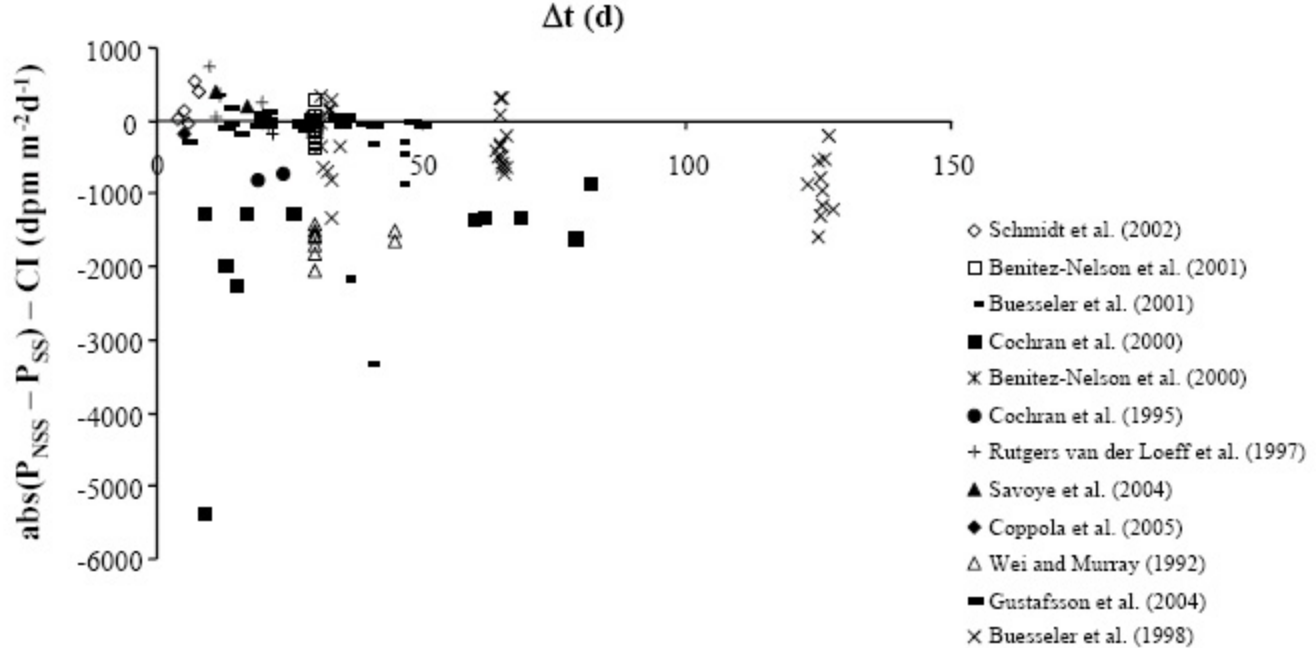
Δt (d)
abs(P_NSS – P_SS) – CI (dpm m-2d-1)
1000
0
-1000
-2000
-3000
-4000
-5000
-6000
0
50
100
150
Schmidt et al. (2002)
Benitez-Nelson et al. (2001)
Buesseler et al. (2001)
Cochran et al. (2000)
Benitez-Nelson et al. (2000)
Cochran et al. (1995)
Rutgers van der Loeff et al. (1997)
Savoye et al. (2004)
Coppola et al. (2005)
Wei and Murray (1992)
Gustafsson et al. (2004)
Buesseler et al. (1998)

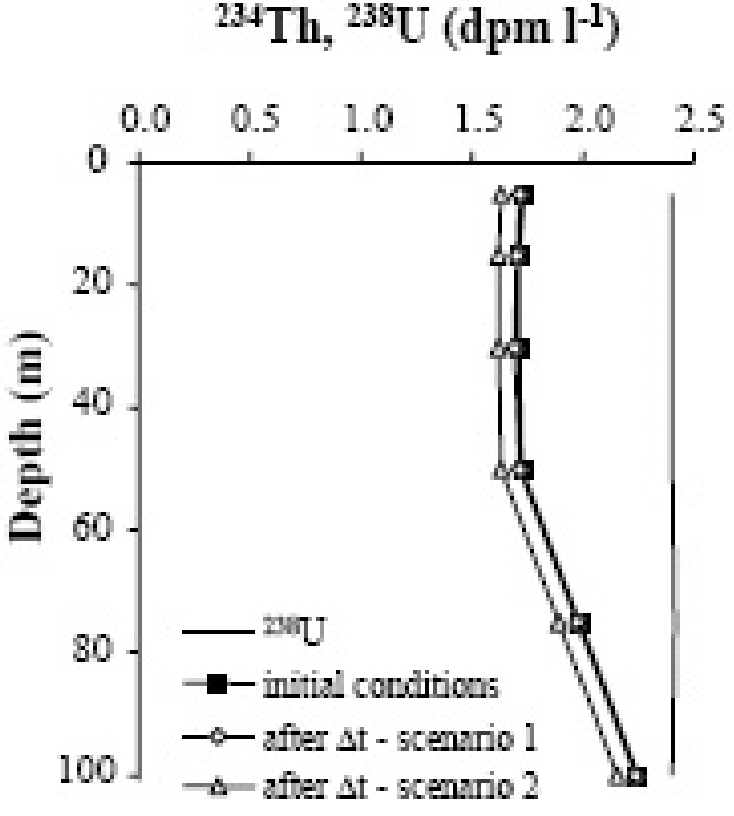
234Th, 238U (dpm l-1)
0.0
0.5
1.0
1.5
2.0
2.5
0
20
40
60
80
100
Depth (m)
238U
initial conditions
after Δt - scenario 1
after Δt - scenario 2

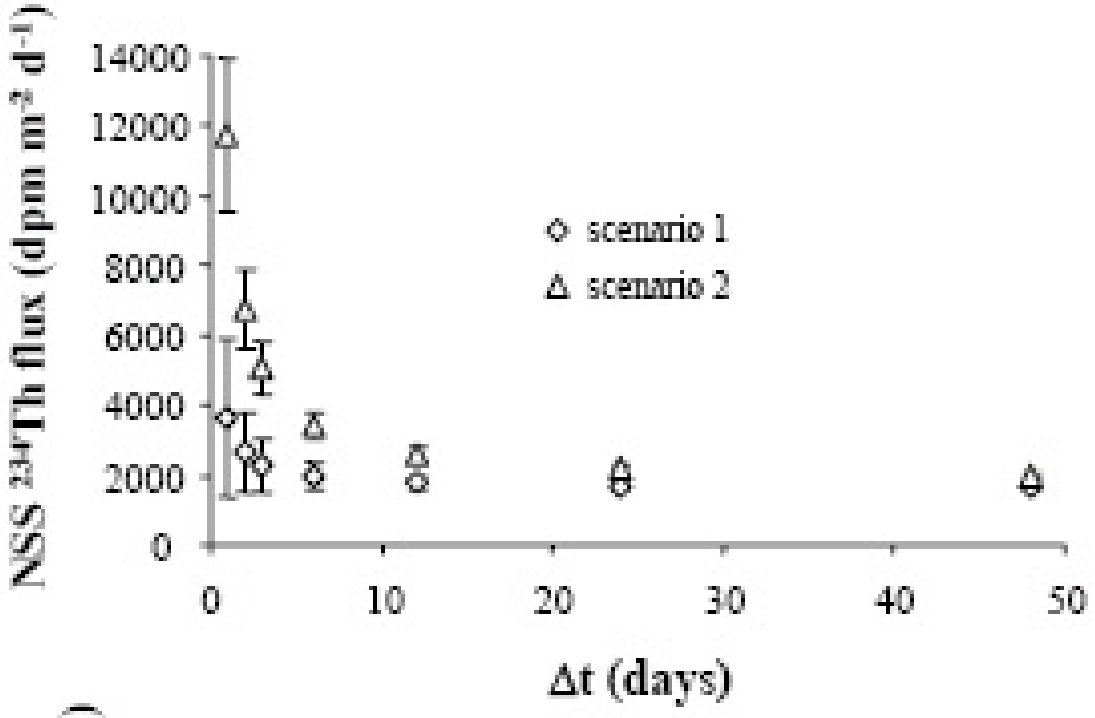
NSS 234Th flux (dpm m-2 d-1)
14000
12000
10000
8000
6000
4000
2000
0
0
10
20
30
40
50
Δt (days)
scenario 1
scenario 2

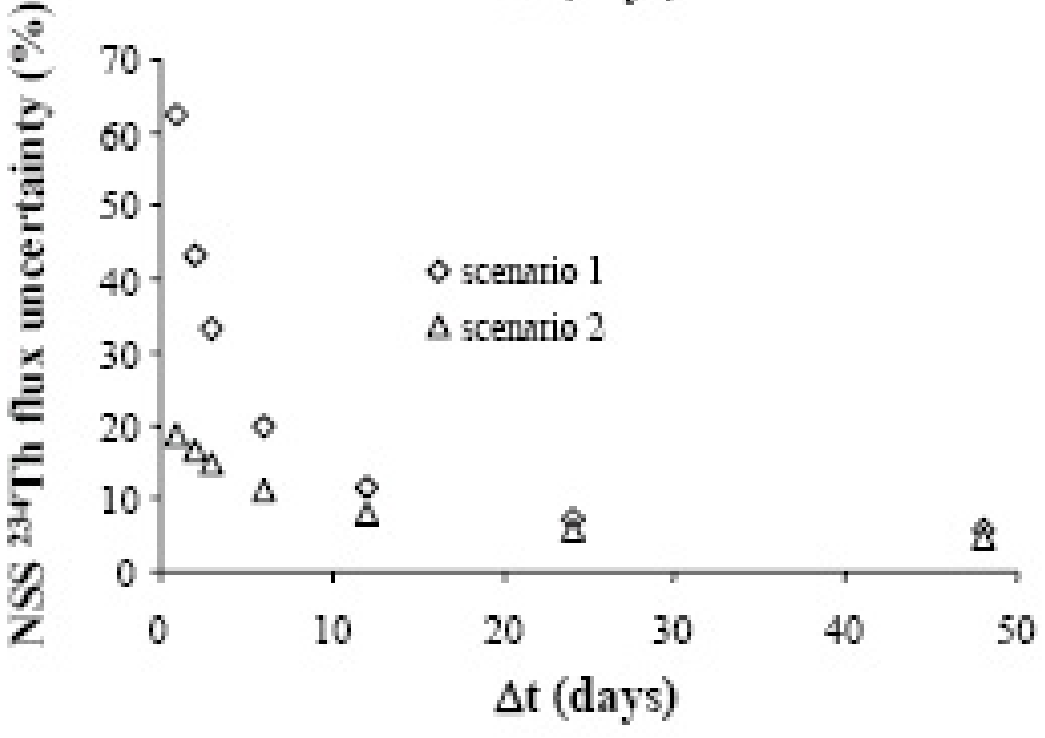
NSS 234Th flux uncertainty (%)
70
60
50
40
30
20
10
0
0
10
20
30
40
50
Δt (days)
scenario 1
scenario 2

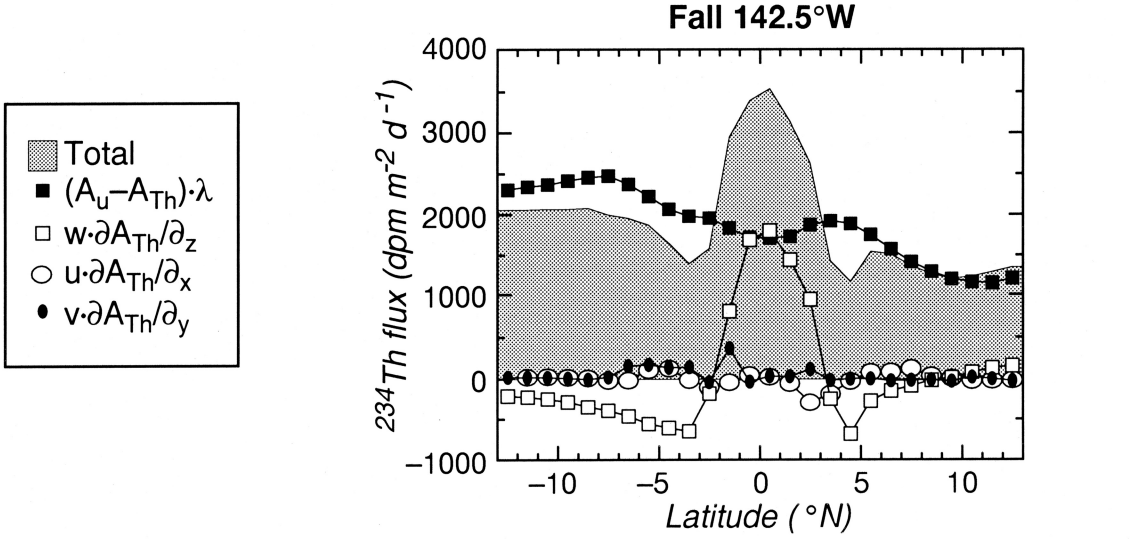
Fall 142.5°W
Total
(Au–ATh)·λ
w·∂ATh/∂z
u·∂ATh/∂x
v·∂ATh/∂y
234Th flux (dpm m-2 d-1)
4000
3000
2000
1000
0
–1000
–10
–5
0
5
10
Latitude (°N)

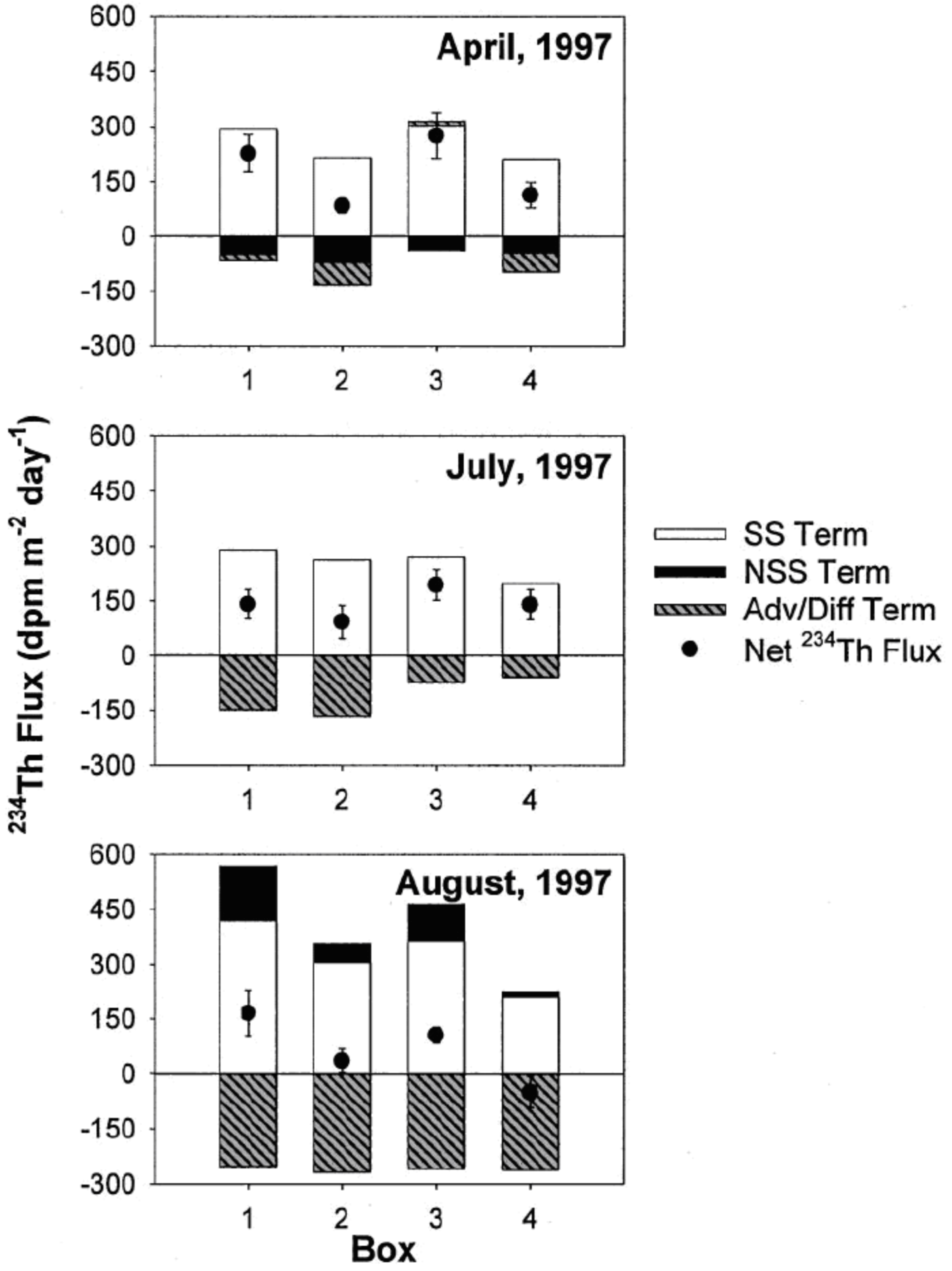
April, 1997
July, 1997
August, 1997
600
450
300
150
0
-150
-300
1
2
3
4
Box
234Th Flux (dpm m-2 day-1)
SS Term
NSS Term
Adv/Diff Term
Net 234Th Flux

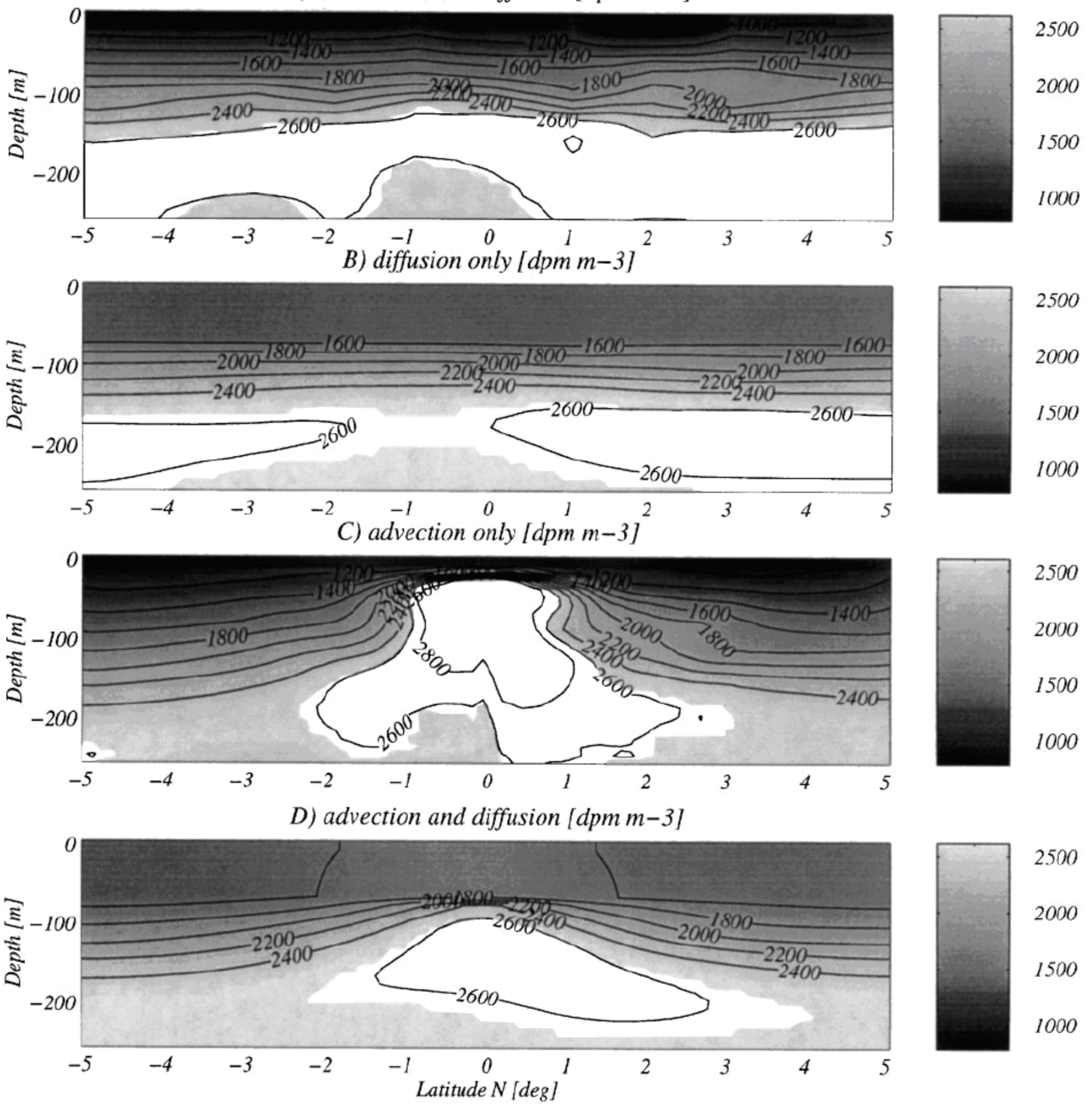
A) no advection or diffusion [dpm m−3]
B) diffusion only [dpm m−3]
C) advection only [dpm m−3]
D) advection and diffusion [dpm m−3]
Depth [m]
0
−100
−200
−5
−4
−3
−2
−1
0
1
2
3
4
5
Latitude N [deg]
2500
2000
1500
1000

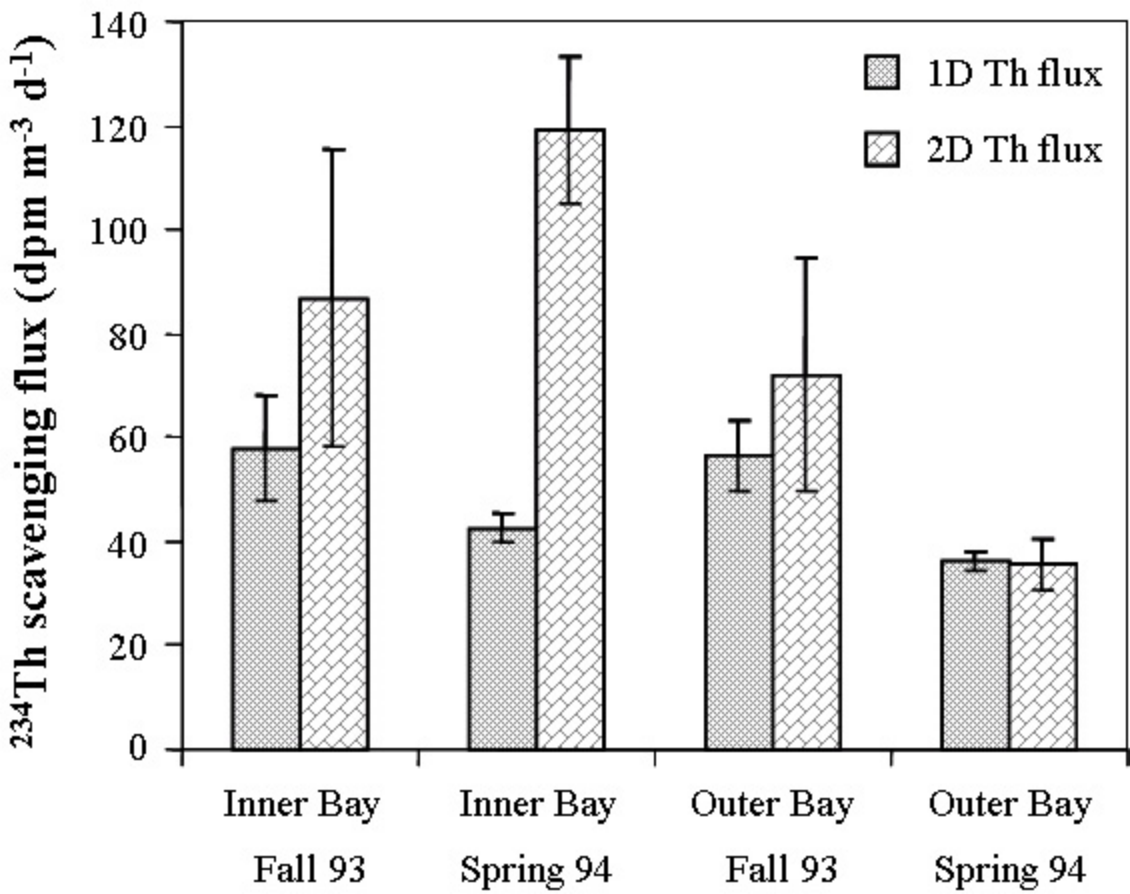
^{234}Th scavenging flux (dpm m^{-3} d^{-1})
140
120
100
80
60
40
20
0
1D Th flux
2D Th flux
Inner Bay
Fall 93
Inner Bay
Spring 94
Outer Bay
Fall 93
Outer Bay
Spring 94

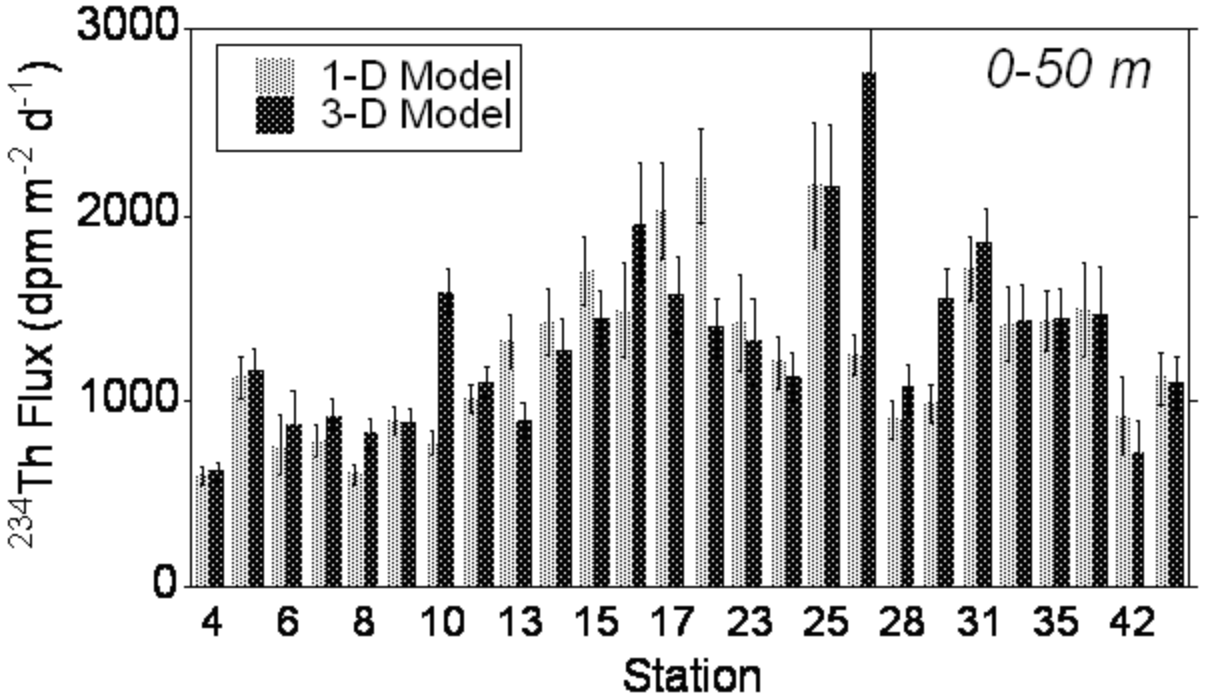
3000
2000
1000
0
1-D Model
3-D Model
0-50 m
234Th Flux (dpm m-2 d-1)
4
6
8
10
13
15
17
23
25
28
31
35
42
Station